Proceedings of ISFOG 2025
5TH INTERNATIONAL SYMPOSIUM ON
FRONTIERS IN OFFSHORE GEOTECHNICS
Nantes, France | June 9-13 2025

ISBN 978-2-85782-758-0

Bending moment profiles as indicators for the lateral stiffness of offshore wind turbines

A. Kheffache*
Ghent University, Ghent, Belgium

B. Stuyts, C. Sastre Jurado
Ghent University, Ghent, Belgium

C. Devriendt
VUB, Brussels, Belgium

*Anis.kheffache@ugent.be

ABSTRACT:
The offshore wind energy sector is experiencing rapid growth, as most of the countries are aiming for a decarbonization of their economy by 2050. Wind turbines located in the Belgian North Sea have been monitored for several years and can serve as a basis for deeper investigation of their in-situ behaviour compared to design expectations.

This paper presents the results of bending moments back analyses on two monitored wind turbine monopiles located in the Belgian North Sea. Two site-specific ground models are established for each wind turbine location. A 3D FEM ABAQUS model is established for each wind turbine, in which the soil is modelled using the hypoplastic constitutive models for sand and clay, which were calibrated using advanced laboratory testing results as well as in-situ test data. The monopiles are subjected to quasi-static operational loads that were derived from the monitoring data. First, the bending moments are computed and compared to the monitored ones for each wind turbine. The bending moments are then linked to the lateral stiffness of each wind turbine. Results are discussed and the possible effect of scour protection is highlighted.
Keywords: Offshore geotechnics; monitoring; wind energy; bending moment; stiffness.

1 INTRODUCTION

Monopiles represented 81% of the total installed foundations for offshore wind turbines (OWTs) in 2019 (WindEurope, 2020). The number of monopile-supported OWTs is expected to have slightly dropped according to newly published reports (Musial et al., 2023). Nonetheless, despite the fast innovation in the OWT sector, monopiles are still expected to be the preferred support structures for OWTs, even in deep waters (up to 60 m depth), mainly due to an already established and robust supply chain.

Monitoring of offshore wind turbines can provide useful insight, which can be used by designers to challenge design assumptions. Kallehave et al. (2015) presented two use cases of monitoring data on OWTs to extend their lifetime by 88% by re-evaluating the fundamental frequency f_0. A total of 20 to 25% reduction of the total steel tonnage was achieved in another wind farm.

In this work, two wind turbine monopiles located in the Belgian North Sea are studied. The monitored bending moments on both monopiles are back-calculated using 3D FEM models. The effect of soil stiffness G_{max} is then established on both the bending moments and the lateral rotational stiffness of both monopiles. The link between lateral stiffness, bending moments and the possible scour protection effects is highlighted.

2 OFFSHORE WIND INDUSTRIAL TRENDS

Offshore wind turbines are dynamic structures for which the fatigue lifetime is an important design factor. OWTs are designed following the soft-stiff approach, where their natural frequency f_0 should fall within a range of forcing frequencies, namely the 3P frequency range and the 1P/wave frequency range at the upper and lower side of the frequency spectrum respectively, P being the rotor's frequency.

Measurements of the natural frequency of OWTs across multiple wind farms reveal a global shift of f_0 towards the wave frequency range (Figure 1). This shift is associated with the ever-increasing structural mass associated with the increase in wind turbines rated power. Moreover, future wind farms will be developed in deeper waters, resulting in longer monopiles, which will enhance the shift even further. In light

of these observations, the accurate stiffness prediction of OWTs is more critical than ever. In design, the soil is generally the main source of uncertainty, which makes an accurate prediction of OWTs stiffness a rather difficult task, thus the need for numerical models that are accurately tuned to capture the overall OWTs stiffness.

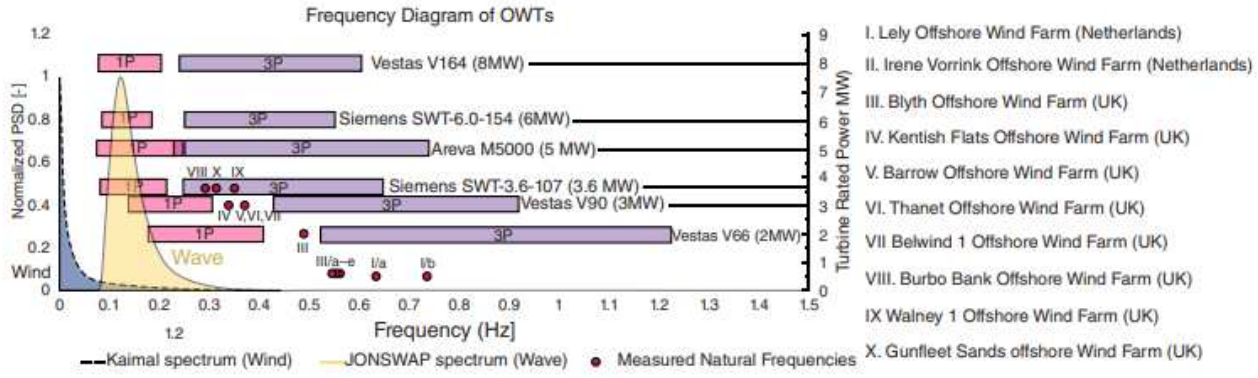

Figure 1. Evolution of the natural frequency of OWTs across multiple wind farms (Bhattacharya, 2019)

3 SITE CONDITIONS

3.1 Monopiles

The studied wind turbine monopiles are located in two different wind farms across the Belgian North Sea. The monopiles are monitored using different monitoring devices such as fibre Bragg Gratings (FBGs) that record the strains along the monopile at predefined depths. The strain measurements can then be transformed to stress and then to bending moments in the fore-aft (FA) and side-side (SS) directions, knowing the main wind direction. The wind turbines are also equipped with SCADA system that records the performance of each wind turbine. Both monopiles geometries are given in the following table:

Table 1.Geometry of the monopiles WTG-A and WTG-B

	h (m)	L (m)	t (mm)	Water depth (m)	D (m)
WTG-A	37	29.9	57-95	32	5
WTG-B	39.9	32.95	55-81	33.9	7.4

where h is the stick-up length (eccentricity from mudline), L is the embedded length, t is the monopile's wall thickness and D is the monopile's diameter.

3.2 Soils

Both studied monopiles are embedded in multilayered soil mediums. The top layers generally consist of medium-dense to dense quaternary sand layers that overlay an over-consolidated tertiary clay layer.

The cone tip resistance measured during cone penetration test at the exact wind turbines locations are shown in Figure 2.

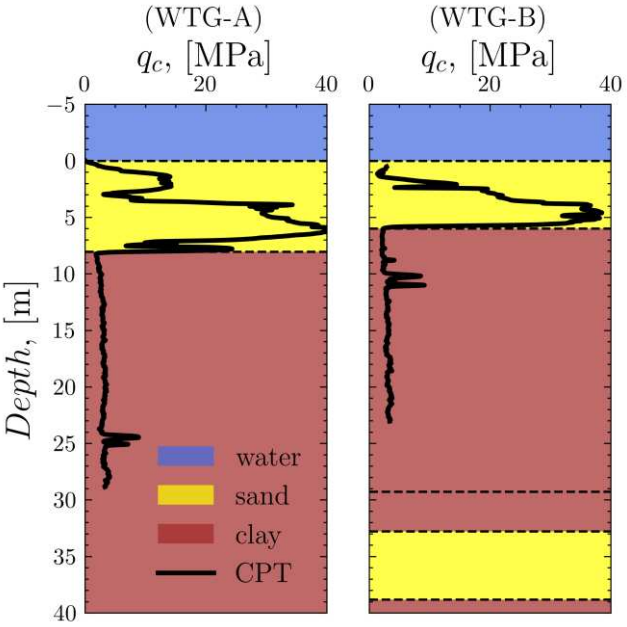

Figure 2. CPTu and soil layering at each wind turbine monopile location.

The 3D FEM ABAQUS model is shown in Figure 3. Only half of the model is simulated, taking advantage of the symmetry in the y direction. Two different model sizes have been used, due to the difference in monopile diameter.

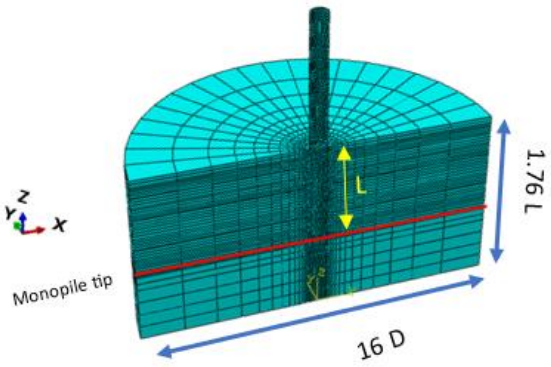

Figure 3. Abaqus 3D numerical model of the soil and monopile

3.3 Loads

The quasi-static wind-induced loads were derived from the monitoring data during normal operational conditions of the wind turbines and were reported directly at the head of the monopile. A more detailed explanation is given in Kheffache et al. (2024).

3.4 Soil modelling

The sand and clay layers were modelled using the hypoplastic constitutive models for sand and clay (Mašín, 2013; von Wolffersdorff, 1996). These models were selected mainly due to the control that they confer over soil stiffness and it's degradation. The constitutive models were previously calibrated in other works (Kheffache et al., 2024).

3.5 Interface modelling

The soil-pile interface is modelled using the ABAQUS general contact algorithm. The tangential contact was assigned a Mohr-Coulomb friction coefficient of 0.5, while the normal contact was assigned a "hard contact" behaviour.

3.6 Parametric studies on soil stiffness G_{max}

The parametric studies performed in this work are focused on the effect of soil stiffness on bending moments. The soil stiffness profile is established at each wind turbine location using the CPTu test results at each location, using the Robertson & Cabal (2015) correlation. The upper and lower bound stiffness profiles have also been established on the upper sand layer, in order to investigate their effect on the simulated bending moment profiles (Stuyts, 2023). The lower layers are always assigned the best-estimate G_{max} profiles, as shown in Figure 4.

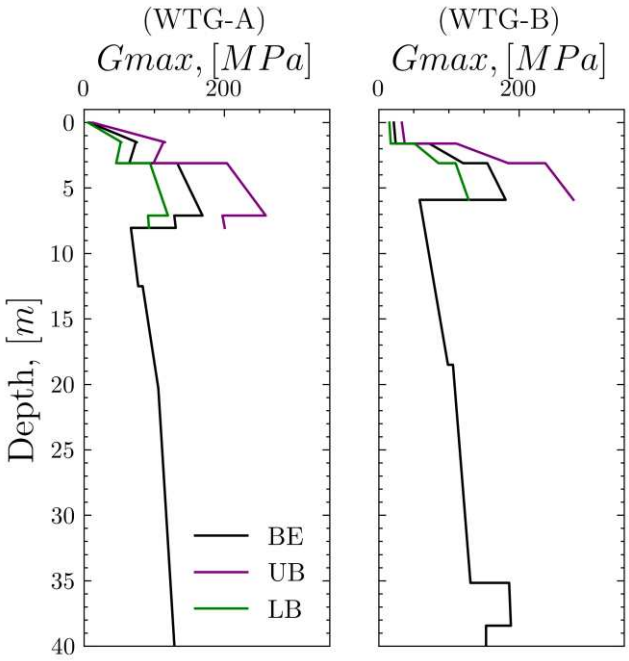

Figure 4. Adopted stiffness profiles at each wind turbines location, as interpreted from CPTu tests. An upper and lower bounds established on the top sand layers.

The $G_{max,1D}$ variable represents the average of G_{max} over the upper one diameter depth, where most of the stresses are transferred from the monopile to the soil under lateral loading. It is introduced in order to numerically investigate the effect of soil stiffness. The different $G_{max,1D}$ values at each wind turbine location are given in the following table:

Table 2. Upper bound, best estimate and lower bound $G_{max,1D}$ at each wind turbine location.

	WTG-A			WTG-B		
	UB	BE	LB	UB	BE	LB
$G_{max,1D}$ (MPa)	141	93	65	152	104	76

4 RESULTS AND DISCUSSIONS

4.1 Simulated and monitored bending moment profiles

The bending moment profile corresponding to the highest monitored load intensity for WTG-A is shown in Figure 5, for different soil stiffness profiles. The bending moments are normalized by the single highest moment value out of the four curves, which corresponds to the moment induced by a lower bound G_{max} profile, at a normalized depth z/D of 0.25 (green curve in Figure 5). It can be seen that the monitored bending moments are overestimated by all the simula-

tions. An increase and a decrease of soil stiffness towards the upper bound and lower bound values (in the top one-pile diameter region) leads to a reduction and augmentation of the bending moment respectively, which allows to establish the effect of soil stiffness on the bending moments under lateral loads (Note that this observation may change under displacement controlled analyses). The same trends were observed for WTG-B, but are not shown here for brevity. It should be pointed that although increasing soil stiffness leads to the decrease in the mismatch, the bending moment profile is still higher than what is monitored.

The mismatch between the monitored and computed bending moments at each sensor depth is quantified using the mean relative error (MRE), which is defined using the following equation:

$$MRE_M = \frac{1}{n}\sum_{i=0}^{n-1}\frac{M_m^{z,i}-M_s^{z,i}}{M_m^{z,i}} \qquad (1)$$

where $M_m^{z,i}$ and $M_s^{z,i}$ are the monitored and simulated moments at sensor depth z for the i-th load case, and n is the total number of load cases for each wind turbine. Negative and positive values of MRE translate into an overestimation and underestimation of the monitored bending moments by the simulated ones respectively. The calculated MRE values are shown in Figure 6. It can be seen that an increase of soil stiffness leads to the decrease in the MRE, which is a decrease of the mismatch between monitored and simulated bending moments, at both WTG locations. It is however clear that the MRE values are all negative, translating an overestimation of the simulated bending moments (simulated bending moments are higher than the monitored ones).

The GMRE value; which is defined as the mean of the MRE values that were calculated at each sensor depth for each wind turbine; is used to obtain a single value to quantify the mismatch between the simulated and monitored bending moments. Similarly to the MRE, a negative and positive value of GMRE translates an over-and-underestimation of the monitored bending moments respectively. It can be seen from Figure 7 that for both WTG, increasing soil stiffness $G_{max,1D}$ from lower bound to upper bound, passing by the best-estimate profile, decreases the GMRE values from -14.2 to -9.8% and from -4.6 to -1.10% for WTG-A and WTG-B respectively. The increase in soil stiffness reduces the bending moments, getting them closer to the monitored ones. Similarly to the MRE, the GMRE values are also negative, translating an overestimation of simulated bending moments.

The wind turbine's stiffness is controlled in a great part by the inner characteristics (bending stiffness EI), but also by the soil stiffness G_{max}, which is often also the main source of uncertainty. The link between soil stiffness and the lateral stiffness of both WTGs is investigated next.

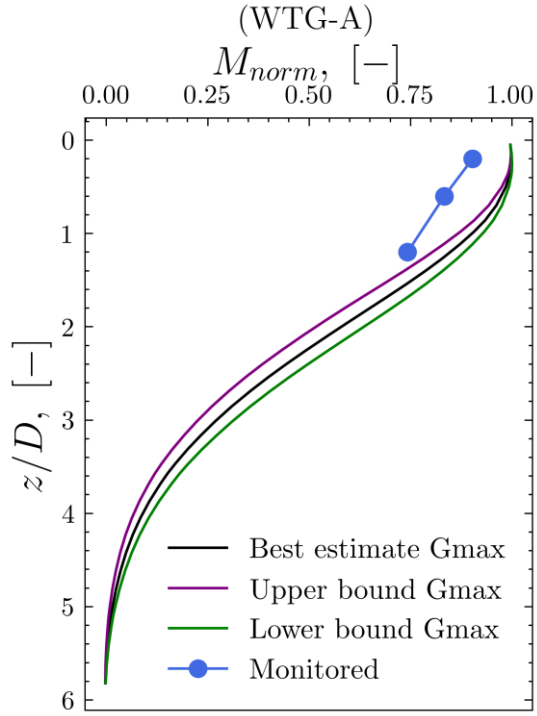

Figure 5. Monitored and simulated bending moment profiles corresponding to the upper, best-estimate and lower bound stiffness profiles for WTG-A. Bending moments are normalized by the moment at z/D of 0.25 induced by a lower bound G_{max} profile.

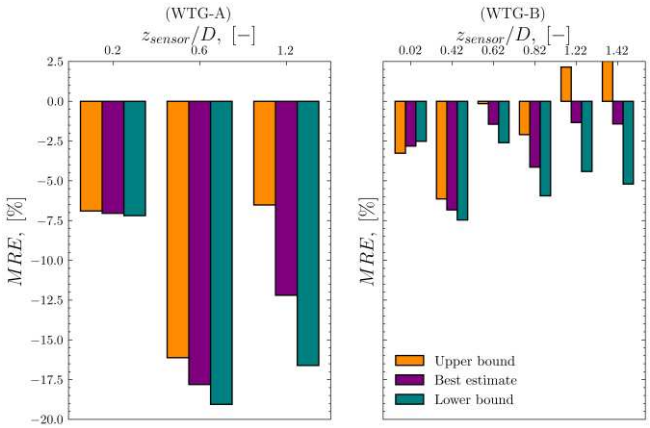

Figure 6. MRE values for WTG-A and WTG-B for different sensor depths.

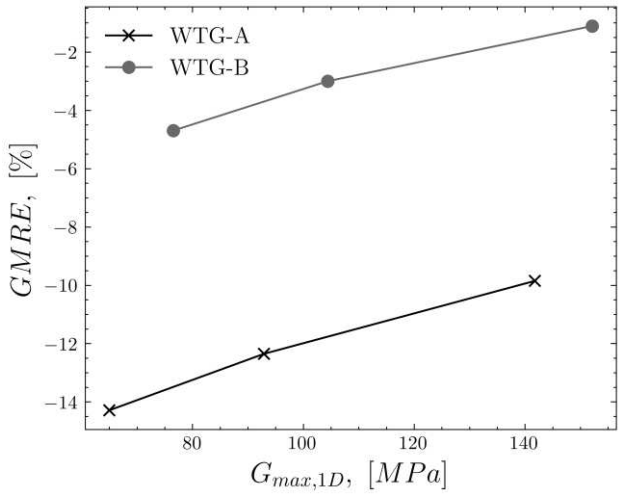

Figure 7. GMRE for WTG-A and WTG-B, considering different soil $G_{max,1D}$ values (lower, best estimate and upper bound)

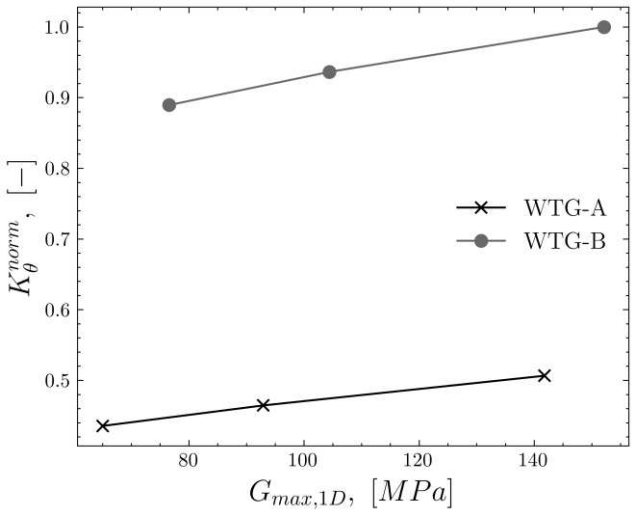

Figure 8. Normalized rotational stiffness values considering different soil stiffness profiles ($G_{max,1D}$).

4.2 Stiffness

The effect of soil stiffness on the lateral rotational stiffness of the wind turbine monopile is further investigated.

The mudline lateral K_L vertical K_v, rotational K_θ, and coupled $K_{\theta L}$ stiffnesses are useful to get a single-value quantifier for the stiffness of offshore wind turbines. The rotational stiffness has the most influence on the natural frequency of wind turbines as it was shown by Bhattacharya (2019), and it will be used in what follows. The mudline rotational stiffness is defined according to the following equation:

$$K_\theta = \frac{M}{\theta} \qquad (2)$$

where M is the moment at mudline level that corresponds to a very small pile rotation at mudline level θ. The K_θ values are normalized by the highest simulated value (corresponding to WTG-B with an upper bound stiffness profile). It can be seen from Figure 8 that similarly to the GMRE trends, increasing the soil stiffness from a lower to an upper bound leads to the increase of K_θ^{norm} from 0.43 to 0.5 and from 0.88 to 1 for WTG-A and WTG-B respectively. The increase of soil stiffness leads to the increase of the lateral stiffness of both wind turbines, which in turn leads to the decrease of the bending moments. The highest K_θ^{norm} values for WTG-B are the result of a higher bending stiffness EI.

4.3 Discussions

It can be seen from Figures 6 and 7 that the MRE and GMRE values are higher for WTG-A compared to those computed for WTG-B, translating a more pronounced mismatch. Having established the effect of soil stiffness on the lateral stiffness, Figure 9 links both the lateral stiffness and the GMRE, where it can be seen that an increase in K_θ^{norm} automatically leads to a decrease of GMRE in absolute value, which is essentially a decrease of the mismatch between the simulated and monitored bending moments.

This leads to deduce that the in-situ wind turbines WTG-A and B are laterally stiffer than what is modelled in this work, and the reason for the mismatch in bending moments is most likely a result of mismatch in lateral stiffness. WTG-A was surrounded by a 1.5 m thick scour protection system that was around two times thicker than that of WTG-B (0.7 m). In the literature, scour protection systems were seen to increase the natural frequency of offshore wind turbines (Mayall et al., 2025; Winkler et al., 2023). The effect of scour protection on the overall stiffness of offshore wind turbines seems to be the missing contribution in the numerical model.

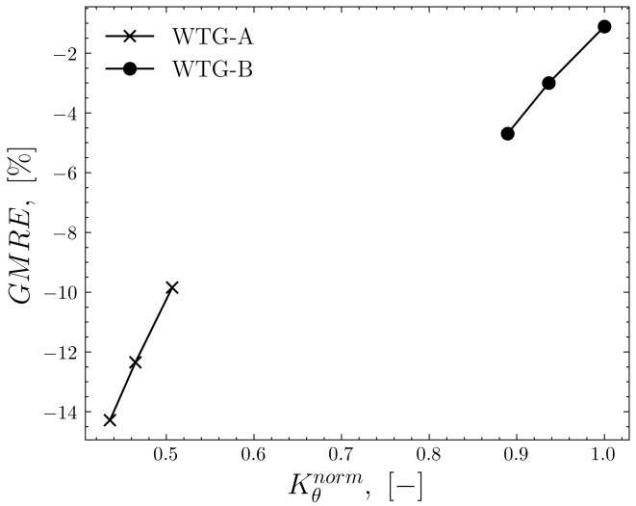

Figure 9. Relation between GMRE and the lateral rotational stiffness of the wind turbines

5 CONCLUSIONS, RECOMMENDATIONS AND FUTURE WORK

In this work, two offshore wind turbine monopiles located in two different wind farms in the Belgian North sea, were comparatively investigated and back calculated using 3D FEM models. Soil stiffness (G_{max}) at each monopile location were linked to the monitored bending moment profiles and mudline rotational stiffness by highlighting the effect of upper, best-estimate and lower bound soil stiffness profiles. The main findings can be summarized as follows:

- The numerical models over-estimate the bending moments on both monopiles. The lateral stiffness of the studied monopiles is most-likely higher than what is modelled.
- Although an increase in soil stiffness reduces the mismatch, the uncertainty on the adopted G_{max} profile at both monopiles locations is not enough to explain the observed mismatch in bending moments (and natural frequency by extension).
- The mismatch in bending moments for WTG-B is lower than for WTG-A, which is most likely related to a stronger stiffening effect at WTG-A compared to WTG-B, possibly due to a thicker scour protection system.
- The scour protection is most-likely contributing to an increase in the lateral stiffness of OWTs, by increasing the soil stiffness (as a result of increased effective stress), and by lowering the free monopile length (additional fixity at the mudline level). It should be taken into account to reduce the mismatch between what is modelled and what is measured in-situ (monitored)

Scour protection systems are generally never taken into account in the design. Future works are going to be focused on including the scour protections and their effect in the numerical models.

AUTHOR CONTRIBUTION STATMENT

A. Kheffache: Formal Analysis, Writing- Original draft, Software, Methodology. **B. Stuyts**: Supervision, Data curation. **C. Sastre Jurado**: Data curation. **C. Devriendt**: Project administration

ACKNOWLEDGEMENTS

The authors would like to acknowledge the support of the Belgian Ministry of Economic Affairs through the EFT project WINDSOIL project. The Support of VLAIO through the De Blauwe Cluster SBO SOILT-WIN project is also acknowledged.

REFERENCES

Bhattacharya, S. (2019). Design of Foundations for Offshore Wind Turbines (1st ed.). Wiley. https://doi.org/10.1002/9781119128137

Kallehave, D., Byrne, B. W., LeBlanc Thilsted, C., & Mikkelsen, K. K. (2015). Optimization of monopiles for offshore wind turbines. Philosophical Transactions of the Royal Society A: Mathematical, Physical and Engineering Sciences, 373(2035), 20140100. https://doi.org/10.1098/rsta.2014.0100

Kheffache, A., Stuyts, B., Sastre Jurado, C., Weijtjens, W., Devriendt, C., & Troch, P. (2024). Advanced simulations of monitored wind turbine monopiles located in the Belgian North Sea under operational quasi-static loading. Ocean Engineering, 311, 118914. https://doi.org/10.1016/j.oceaneng.2024.118914

Mašín, D. (2013). Clay hypoplasticity with explicitly defined asymptotic states. Acta Geotechnica, 8(5), 481–496. https://doi.org/10.1007/s11440-012-0199-y

Mayall, R. O., Burd, H. J., McAdam, R. A., Byrne, B. W., Whitehouse, R. J. S., Heald, S. G., & Slater, P. L. (2025). Numerical Modeling of the Influence of Scour and Scour Protection on Monopile Dynamic Behavior. Journal of Waterway, Port, Coastal, and Ocean Engineering, 151(1), 04024019. https://doi.org/10.1061/JWPED5.WWENG-2027

Musial, W., Spitsen, P., Duffy, P., Beiter, P., Shields, M., Hernando, D. M., Hammond, R., Marquis, M., King, J., & Sriharan, S. (2023). Offshore Wind Market Report: 2023 Edition.

Robertson, P., & Cabal, K. L. (2015). Guide to Cone Penetration Testing. R:\Zotero\CA Technical references\2015 Robertson and Cabal - Guide to Cone Penetration Testing.pdf

Stuyts, B. (2023). Improved soil-structure interaction for offshore monopiles based on in-situ monitoring data [PhD Thesis]. Vrije Universiteit Brussel.

von Wolffersdorff, P.-A. (1996). A hypoplastic relation for granular materials with a predefined limit state surface. Mechanics of Cohesive-Frictional Materials, 1(3), 251–271. https://doi.org/10.1002/(SICI)1099-1484(199607)1:3<251::AID-CFM13>3.0.CO;2-3

WindEurope. (2020). Offshore Wind in Europe: Key trends and statistics 2019. https://windeurope.org/wp-content/uploads/files/about-wind/statistics/WindEurope-Annual-Offshore-Statistics-2019.pdf

Winkler, K., Weil, M., Sastre Jurado, C., Stuyts, B., Weijtjens, W., & Devriendt, C. (2023). Quantifying the effect of rock armour scour protection on eigenfrequencies of a monopile supported OHVS. Journal of Physics: Conference Series, 2626, 012039. https://doi.org/10.1088/1742-6596/2626/1/012039